Highlights

(1) An assessment model for solar energy accommodation capability is proposed to determine the solar accommodation potential of the district integrated electrical and heating systems with the consideration of the transmission delay of the district heating network.

(2) The solar collector plays a crucial role in enhancing the solar energy accommodation capability.

(3) The transmission delay characteristics of the DHN can be fully utilized by adjusting the supply temperature of energy stations in a reasonable range to exceed the restriction of the heat load on a typical summer day.

(4) An appropriate increase in solar collector capacity will cause the phenomenon of solar curtailment, but it will also help to promote solar energy accommodation.

(5) For the system in which the solar collector plays a dominant role in solar energy accommodation, the influence of the thermal energy storage on the solar energy accommodation capability is more significant than that of the electric energy storage.

Title：Assessment of the solar energy accommodation capability of the district integrated energy systems considering the transmission delay of the heating network

Author names and affiliations：

Wei Wei[a], Jingwen Wu[a], Yunfei Mu[a,*], Jianzhong Wu[b], Hongjie Jia[a]

[a] Key Laboratory of Smart Grid of Ministry of Education, Tianjin University, Tianjin 300072, China

[b] School of Engineering, Cardiff University, Cardiff, CF24 3AA, UK

* Corresponding author.

E-mail addresses: weiw@tju.edu.cn (W. Wei); jingwwu@tju.edu.cn (J. Wu); yunfeimu@tju.edu.cn (Y. Mu); wuj5@cardiff.ac.uk (J. Wu); hjjia@tju.edu.cn (H. Jia)

Abstract：

With the rapid development of global solar energy applications in recent years, it is crucial to establish a scientific assessment method for solar energy accommodation capability to formulate a rational solar energy utilization scheme. With consideration of two typical solar utilization technologies, photovoltaic and solar thermal collecting technology, and the difference between the energy grades of electricity and heat, new assessment indicators are proposed to investigate the accommodation capability of solar energy. Based on the proposed assessment indicators, an assessment model is carried out to determine the solar accommodation capability of district integrated electrical and heating systems (DIEHSs) considering transmission delay of district heating network (DHN), which can inform the development of an optimal solar accommodation scheme. The effectiveness of the assessment model is verified through a DIEHS consisting of an IEEE 33-bus system and a DHN in China. Finally, specific strategies for enhancing solar energy accommodation capability are given by analyzing the influences of transmission delay of DHN, operating temperature range, solar energy curtailment rate, and energy storage on solar energy accommodation capability.

Keywords: Solar energy accommodation capability, Integrated energy system, Transmission delay of district heating network, Photovoltaic, Solar collector

1. Introduction

With the rapid development of economy and society and the continuous progress of energy industry technology, the wave of promoting the development of renewable energy is gradually sweeping across the world [1]. As a potential renewable energy resource, solar energy will play an important role in the future global energy structure [2]. From 2015 to 2019, global solar energy consumption increased by 176% from 2.34 EJ to 6.45 EJ [3]. However, as the use of solar energy equipment has increased, most countries have experienced challenges due to the unreasonable solar energy consumption and the serious solar energy curtailment, which limits the maximum accommodation and utilization of solar energy [4]. To make full use of solar energy, it is necessary to establish a scientific assessment method for solar energy accommodation capability to formulate a reasonable accommodation scheme.

For the past few years, considerable efforts have been made to study on the general methodology for assessment solar potential. Ref. [5-7] analyzed the solar energy resource in selected areas based on geographic information system (GIS), and then the technological and economic potentials of solar energy were evaluated with photovoltaic (PV) parameters, which helped to determine the exclusion and

inclusion zones. The solar energy potential evaluated in such studies are relatively optimistic without considering the influence of other energy supply equipment and the energy networks on the installation of PV. With comprehensive consideration of specific energy systems including various energy supply equipment, energy conversion equipment, and energy storage equipment, Ref. [8] conducted the simulation and evaluation of solar energy accommodation under different penetration points of renewable energy sources. Ref. [9] took the transient stability constraints of power networks into consideration in the assessment of solar energy accommodation, and investigated the accommodation capability constraints of the grid-connected photovoltaic generation system and the recommendations to improve the solar energy accommodation capability.

The researches mentioned above are restricted to the single accommodation in form of PV. Besides, the other common solar utilization technologies include solar thermal collecting technology, hybrid photovoltaic/thermal (PVT) technology, etc. In recent years, solar collector technology has been disseminated and incentivized in low-carbon heating and large-scale district heating [10-12]. PVT has a favorable application and development in building energy consumption [13]. Multi-form solar utilization provides ideas of improving the level of the solar energy accommodation. Ref. [14] pointed out that integrated solar energy systems of PV and solar water heating facilities is the appropriate approach for wide-scale solar energy applications. Ref. [15] indicated that it was more conducive to solar potential exploitation to develop different accommodation modes according to the building types, which was verified by the proposed evaluation method of solar energy potential based on the PV and solar thermal collecting system.

Multi-form solar energy accommodation involves multiple energy sources such as electricity and heat, the dependent system belongs to the category of integrated energy systems (IESs). The IES carries various energy coupling equipment and energy storage equipment, etc. It can effectively realize the organic integration of multi-form solar energy accommodation and promote the accommodation capability through the coordination and complementarity among multi-energy carriers [16,17]. Recently, a considerable number of studies have been carried out on this topic. Ref. [18] indicated that renewable energy accommodation could be promoted by improving the operational flexibility of the system through combined heat and power (CHP) units, electric boilers (EBs), electric energy storage (EES) systems, thermal energy storage (TES) systems, and spinning reserves. A case study of a specific system including CHP, heat pumps (HPs) and TES is given in Ref. [19] to demonstrate the potential of integrated electrical and heating systems in the renewable energy accommodation. Ref. [20] concluded from the evaluation of the solar energy accommodation capacity of IESs that the comprehensive application of PV and solar collectors (SCs), combined with the CHP, gas boilers (GBs) and other energy conversion equipment, can effectively improve the solar energy accommodation capacity of IESs.

The above-mentioned researches are mostly limited to the integrated solar energy consumption of buildings, and few of them focusing on the IES including energy networks do not consider the differences in time-scale characteristics in the research of solar energy accommodation involving multi-energy carriers [20-22]. In reality, the IES is essentially a complex system with multiple time scales as it involves different energy carriers such as electricity and heat. Transmission delay of heating networks and gas networks cannot be ignored especially for operation, analysis, and evaluation of district and above-scale IESs [23]. Moreover, the accommodation of solar energy could be further improved if the multiple time-scale characteristics of district IES can be used reasonably to realize operation optimization.

In addition to the specific methods and influencing factors of solar energy accommodation assessment, indicator establishment of the solar energy accommodation capacity is another emphasis of

the assessment process. Some researches try to establish representative indicators such as the actual total output of solar energy equipment [4,6,24], the installed capacity of solar energy equipment that can be accommodated by the systems [9,20], the ability of a given system to flexibly integrate fluctuating solar energy output [8,25] and the annual investment cost of solar energy equipment considering economy [6,8]. However, the researches mentioned above also do not consider the multiple forms of the solar energy accommodation, which brings about the problem of how to evaluate different energy carriers for the indicators establishment of the solar energy accommodation capacity. There are two main evaluation criteria for electric and thermal energy in solar energy accommodation. The first one is energy evaluation, taking electric and thermal energy as equivalent based on the first law of thermodynamics [26]. It reflects the quantity of different energy carriers and focuses on the assessment of energy consumption, the economy, and environmental protection. The second one is exergy evaluation based on the second law of thermodynamics, which uses the exergy to reveal the difference in the energy grades of energy carriers. It puts the emphasis on the energy quality and the efficiency evaluation of equipment and IESs [26,27]. Let us take the integrated solar energy systems of the PV and SC as an example. The conversion efficiency of the SC is higher than that of PV, but it does not mean the SC is a better solar accommodation equipment than the PV. The electricity produced by the PV belongs to high-quality energy, while the heat produced by the SC belongs to low-quality energy. Taking into account the difference in the energy grade between heat and electricity, it is more reasonable to establish indicators of the solar energy accommodation capacity based on energy quality in IESs.

According to the existing problems mentioned above, this paper focuses on the assessment of the solar energy accommodation capability of the district integrated electrical and heating systems (DIEHSs). New evaluation indicators of solar energy accommodation capability are proposed considering the energy grade of electrical and thermal carriers of solar energy accommodation. Based on the impacts of the transmission delay of district heating network (DHN), and the coordinated operation of the DIEHS including heat-electric coupling equipment and energy storage equipment, an assessment model of solar energy accommodation capability is developed to provide the optimal utilization pattern of solar energy for DIEHSs. In the case study, the influences of operating temperature range, solar curtailment rate and energy storage equipment on the solar energy accommodation capability are drilled down.

2. Modelling the DIEHSs

A DIEHS, which consists of power distribution networks (PDNs), DHNs, energy stations (ESs), and distributed energy sources, supplies energy to users within a town or city, a district area, or a community. A typical structure of a DIEHS is shown as Fig. 1. As the power transmission link, the PDN connects the grid, ESs, and power users. The DHN is the heating transmission hub of heat users and centralized heat sources. ESs can accommodate multiple energy supply equipment (such as PV, SC, CHP, EB, EES, and TES), providing energy supply for users. Distributed energy sources are located at the end users', whose influences on the district energy supply system are reflected in load characteristics, not considered in this paper. Considering the application situation and market of the solar energy equipment, this paper mainly focuses on PV and SC which are widely used at present, and does not involve PVT.

The mathematical model of each component of the DIES is as follows.

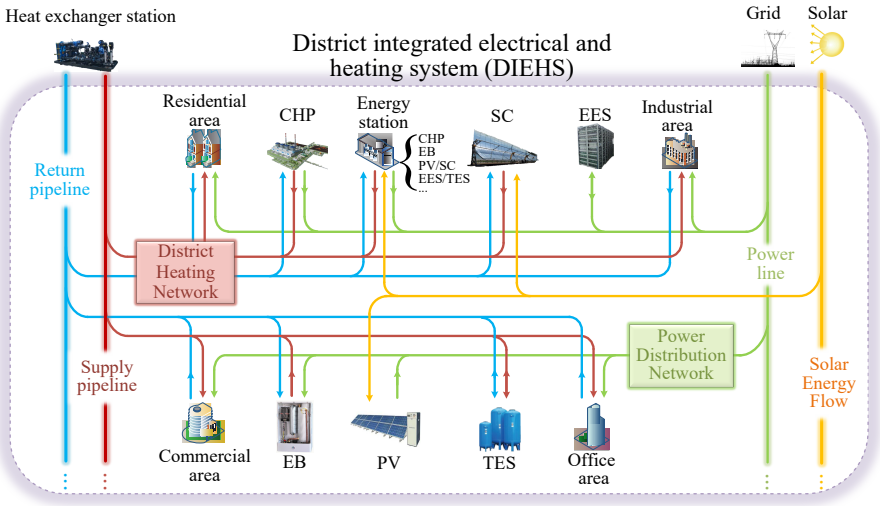

Fig. 1. Diagram of a typical DIEHS

2.1. Transmission delay model and operation constraints of DHN

Traditional heating regulation modes of the DHN contain the quality regulation mode, the quantity regulation mode, etc. The quality regulation mode refers to the operation strategy of constant mass flow and variable temperature supply (CF-VT). The thermal output of ESs is controlled by the supply temperature of the heat sources [28] and the difference between the supply and return temperature is not a relative constant even though there exists the electricity backup. Because of its convenient operation and stable hydraulic regime, CF-VT has become one of the most extensively used regulation modes of DHN in engineering applications. As the hydraulic dynamic process of the DHN is much faster than the thermal dynamic process [23], the mass flow in pipelines can be considered constant under CF-VT in this study. Therefore, the thermal transmission delay characteristic is focused on.

Under the CF-VT mode, the transmission delay model of the DHN can be described as follows.

(1) Node temperature

For node j shown in Fig. 2, the mixture temperature equations of node j in the supply and return pipelines can therefore be described as

$$\sum\nolimits_{i\in\delta^{\mathrm{s}}(j)}(m_{ij}T^{\mathrm{s},t}_{\mathrm{out},ij})=(\sum\nolimits_{k\in\xi^{\mathrm{s}}(j)}m_{jk}+m_{\mathrm{load}\,j})T^{\mathrm{s},t}_{j} \tag{1}$$

$$m_{\mathrm{load}\,j}T^{\mathrm{r},t}_{\mathrm{load},j}+\sum\nolimits_{k\in\delta^{\mathrm{r}}(j)}(m_{jk}T^{\mathrm{r},t}_{\mathrm{out},jk})=(\sum\nolimits_{i\in\xi^{\mathrm{r}}(j)}m_{ij})T^{\mathrm{r},t}_{j} \tag{2}$$

Let us assume that $T'^{t}_{j}=T^{t}_{j}-T^{t}_{\mathrm{a}}$. Divide both sides of the equation by the total mass flow injected into node j in Eqs. (1)–(2), and then Eqs. (1)–(2) can be written as

$$T'^{\mathrm{s},t}_{j}=\sum\nolimits_{i\in\delta^{\mathrm{s}}(j)}(\beta^{\mathrm{s}}_{ij}T'^{\mathrm{s},t}_{\mathrm{out},ij}) \tag{3}$$

$$T'^{\mathrm{r},t}_{j}=\beta^{\mathrm{r}}_{\mathrm{load},j}T'^{\mathrm{r},t}_{\mathrm{load},j}+\sum\nolimits_{k\in\delta^{\mathrm{r}}(j)}(\beta^{\mathrm{r}}_{jk}T'^{\mathrm{r},t}_{\mathrm{out},jk}) \tag{4}$$

$$\beta^{\mathrm{s}}_{ij}=m_{ij}\Big/\sum\nolimits_{i\in\delta^{\mathrm{s}}(j)}m_{ij} \tag{5}$$

$$\beta^{\mathrm{r}}_{\mathrm{jk}}=m_{jk}\Big/(m_{\mathrm{load},j}+\sum\nolimits_{k\in\delta^{\mathrm{r}}(j)}m_{jk}) \tag{6}$$

$$\beta^{\mathrm{r}}_{\mathrm{load},j}=m_{\mathrm{load},j}\Big/(m_{\mathrm{load},j}+\sum\nolimits_{k\in\delta^{\mathrm{r}}(j)}m_{jk}) \tag{7}$$

The finite difference method is applied to deal with the thermal transmission delay character of pipelines. Assuming Δt is the time interval, pipe ij can be approximatively divided into τ_{ij} units with a length of Δl_{ij} according to Δt, as shown in Fig. 3, where τ_{ij} can be calculated by

$$\tau_{ij}=round\left[l_{ij}/\Delta l_{ij}\right] \tag{8}$$

$$\Delta l_{ij} = 4m_{ij}\Delta t \big/ \pi D_{ij}^2 \rho \tag{9}$$

It is known that the thermal process transmits at the speed of the value of the mass flow rates [23]. As a result, the time for the temperature impact of node i on node j is approximatively $\tau_{ij}\Delta t$. With consideration of heat loss, the outlet temperature of pipe ij at time t can be calculated by

$$T'^{\mathrm{s},t}_{\mathrm{out},ij} = T'^{\mathrm{s},t-\tau_{ij}\Delta t}_{i} \exp(-\lambda_{ij} l_{ij} \big/ cm_{ij}) \tag{10}$$

By substituting Eq. (10) into Eq. (3) and assuming $\psi_{ij} = \exp(-\lambda_{ij} l_{ij} \big/ cm_{ij})$, the supply temperature calculation formula at node j can be obtained:

$$T'^{\mathrm{s},t}_{j} = \sum\nolimits_{i\in\delta^{\mathrm{s}}(j)} \beta^{\mathrm{s}}_{ij}\psi_{ij} T'^{\mathrm{s},t-\tau_{ij}\Delta t}_{i} \tag{11}$$

Similarly, the return temperature calculation formula at node j is

$$T'^{\mathrm{r},t}_{j} = a^{\mathrm{r}}_{\mathrm{load},j} T'^{\mathrm{r},t}_{\mathrm{load},j} + \sum\nolimits_{k\in\delta^{\mathrm{r}}(j)} \beta^{\mathrm{r}}_{jk}\psi_{jk} T'^{\mathrm{r},t-\tau_{jk}\Delta t}_{k} \tag{12}$$

In Eqs. (11)–(12), $T^{\mathrm{s},t-\tau_{ij}\Delta t}_{i}$ and $T^{\mathrm{r},t-\tau_{jk}\Delta t}_{k}$ should be replaced by the initial supply temperature at node i and the initial return temperature at node k , respectively, when $t < \tau\Delta t$.

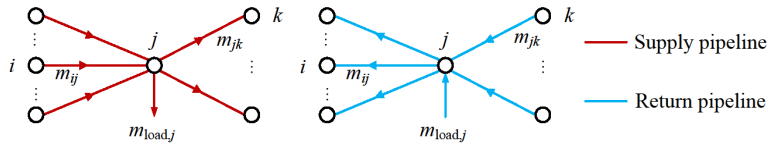

Fig. 2. Diagram of pipe connection at node j

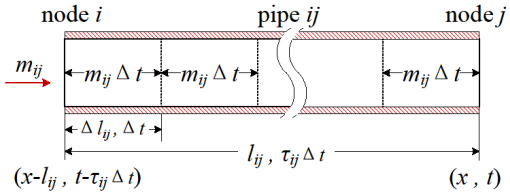

Fig. 3. Vertical diagram of supply pipe ij

(2) Heat loss of pipes

For a pipe unit with a temperature of T and heat transfer coefficient of λ, the heat loss at time t is [29]

$$\Delta H^{t}_{\mathrm{loss}} = \lambda T'^{t} \tag{13}$$

Assume that the temperature of every pipe unit is represented by the average temperature at the inlet and outlet of the pipe unit. According to Eq. (13), the heat loss of pipe ij with start node of node i at time t can be calculated as follows when the trapezoidal integration method is used:

$$H^{t}_{\mathrm{loss},ij} = \lambda_{ij}\Delta l_{ij} \sum\nolimits_{n=1}^{\tau_{ij}} (\psi_{ij}^{(n-1)/\tau_{ij}} T_i'^{t-(n-1)\Delta t} + \psi_{ij}^{n/\tau_{ij}} T_i'^{t-n\Delta t}) \big/ 2 \tag{14}$$

Eq. (14) is applicable to both supply and return pipelines.

(3) Heat source and heat load

The heat power of the source and load at node i and time t can be calculated as follows:

$$H^{t}_{\mathrm{source},i} = cm_{\mathrm{source},i}\left(T^{\mathrm{s},t}_{i} - T^{\mathrm{r},t}_{i}\right) \tag{15}$$

$$H^{t}_{\mathrm{load},i} = cm_{\mathrm{load},i}\left(T^{\mathrm{s},t}_{i} - T^{\mathrm{r},t}_{\mathrm{load},i}\right) \tag{16}$$

The heat power of the source at node i and time t is equal to the thermal output of all the heating equipment:

$$H^{t}_{\mathrm{SC},i} + H^{t}_{\mathrm{CHP},i} + H^{t}_{\mathrm{EB},i} + H^{t}_{\mathrm{TES,D},i} - H^{t}_{\mathrm{TES,C},i} = H^{t}_{\mathrm{source},i} \tag{17}$$

(4) Temperature constraints

For all nodes in the entire DHN at arbitrarily time t, there exists an operating temperature range [30-32]:

$$T^{\mathrm{s,min}} \le T^{\mathrm{s},t}_{i} \le T^{\mathrm{s,max}} \tag{18}$$

$$T^{\mathrm{r,min}} \le T_i^{\mathrm{r},t} \le T^{\mathrm{r,max}} \tag{19}$$

For the return temperature, some researches only restrict the lower limit. In order to study the influence of the variation of the return temperature on the solar energy accommodation capacity, the constraint of the upper limit is also introduced in the model.

Besides, to avoid the reckless impact of the transmission delay of the DHN on the state of the following day, the supply temperature of the heat source at the last dispatch time of each day should be consistent with the temperature at the initial dispatch time:

$$T_i^{\mathrm{s,end}} = T_i^{\mathrm{s,init}} \tag{20}$$

2.2. Model of power distribution network

A Distflow second-order cone model is used to describe the PDN in this paper. For arbitrary bus *j* at time *t*, there exist:

$$\sum\nolimits_{i\in\delta^{\mathrm{e}}(j)}(P_{ij}^t - r_{ij}i_{ij}^t) + P_j^t = \sum\nolimits_{k\in\xi^{\mathrm{e}}(j)} P_{jk}^t \tag{21}$$

$$\sum\nolimits_{i\in\delta^{\mathrm{e}}(j)}(Q_{ij}^t - x_{ij}i_{ij}^t) + Q_j^t = \sum\nolimits_{k\in\xi^{\mathrm{e}}(j)} Q_{jk}^t \tag{22}$$

$$P_j^t + P_{\mathrm{load},j}^t = P_{\mathrm{grid},j}^t + P_{\mathrm{CHP},j}^t + P_{\mathrm{PV},j}^t - P_{\mathrm{EB},j}^t + P_{\mathrm{EES,D},j}^t - P_{\mathrm{EES,C},j}^t \tag{23}$$

$$Q_j^t + Q_{\mathrm{load},j}^t = Q_{\mathrm{grid},j}^t + Q_{\mathrm{CHP},j}^t \tag{24}$$

For arbitrary branch *ij*, there exist

$$u_j^t = u_i^t - 2(r_{ij}P_{ij}^t + x_{ij}Q_{ij}^t) + (r_{ij}^2 + x_{ij}^2)i_{ij}^t \tag{25}$$

$$\left\| 2P_{ij}^t, 2Q_{ij}^t, i_{ij}^t - u_i^t \right\|_2 \le i_{ij}^t + u_i^t \tag{26}$$

$$P_{\mathrm{loss},ij}^t = i_{ij}^t r_{ij} \tag{27}$$

All node voltage and branch current should operate within a safe range:

$$u_{\min} \le u_i^t \le u_{\max} \tag{28}$$

$$0 \le i_{ij}^t \le i_{\max} \tag{29}$$

No power transmission to the grid is allowed in this study because the research emphasizes on the solar accommodation capability of the DIEHS itself. As a result, the power from the grid at node *j* satisfies the following constraint:

$$0 \le P_{\mathrm{grid},j}^t \le P_{\mathrm{grid},j}^{\max} \tag{30}$$

2.3. Equipment models

In accordance with the assessment of solar energy accommodation capability in the DIEHS, the solar energy equipment, heat-electric coupling equipment, and energy storage equipment are the focus of this study.

(1) Solar energy equipment

Solar energy equipment in the DIEHS consists of typical solar power generation equipment, PV, and typical solar thermal collection equipment, SC. The installation area of solar energy equipment is usually limited whether it is the roof or the ground. When the PV and SC are installed in the same area, a competitive relationship appears:

$$0 \le A_{\mathrm{PV},i} + A_{\mathrm{SC},i} \le A_i^{\max} \tag{31}$$

The general model of PV at node *i* and time *t* is as follows [33]:

$$P_{\mathrm{PV},i}^t + P_{\mathrm{cur},i}^t = A_{\mathrm{PV},i} I_i^t \eta_{\mathrm{PV},i} \tag{32}$$

$$P_{\mathrm{PV},i}^t \ge 0, P_{\mathrm{cur},i}^t \ge 0 \tag{33}$$

where $P_{\mathrm{PV},i}^t$ is the actual power generated by the PV to the DIEHS at node *i* and time *t*. $P_{\mathrm{cur},i}^t$ is the curtailed actual power of the PV. $\eta_{\mathrm{PV},i}$ is the conversion efficiency of the PV.

The model of the water heating solar collectors is as follows [34,35]:

$$H_{\mathrm{SC},i}^{t}+H_{\mathrm{cur},i}^{t}=A_{\mathrm{SC},i}I_{i}^{t}\eta_{\mathrm{SC},i} \tag{34}$$

$$H_{\mathrm{SC},i}^{t}\geq 0, H_{\mathrm{cur},i}^{t}\geq 0 \tag{35}$$

where $H_{\mathrm{SC},i}^{t}$ is the heat power generated by the SC to the DIEHS at node i and time t. $H_{\mathrm{cur},i}^{t}$ is the curtailed heat power of the SC [31,36]. $\eta_{\mathrm{SC},i}$ is its conversion efficiency. In the performance study of the SC, the conversion efficiencies contain the instantaneous efficiency and the daily efficiency [37-39]. The instantaneous efficiency is related to the difference between average temperature of the SC and the ambient temperature, greatly influenced by external operating conditions. And there exists a complicated thermodynamic relationship between the average temperature of the SC and heating conditions, internal structures and parameters, ambient temperature, solar irradiation, etc. The daily efficiency takes into account the overall performance of the SC throughout the day and is less affected by the random variation of the operating conditions. The solar energy accommodation capacity studied in this paper pays more attention to the synergy between the SC and the DHN and the PDN, rather than the internal design of the SC, so the daily efficiency is used:

$$\eta_{\mathrm{SC},i}=\eta_{\mathrm{SC},i}^{*}-U_{\mathrm{loss,SC},i}\frac{T_{\mathrm{SC},i}^{\mathrm{init}}-\overline{T_{a}}}{\sum_{t=1}^{N_{\Delta t}}I_{i}^{t}} \tag{36}$$

where $\eta_{\mathrm{SC},i}^{*}, U_{loss}$ are the efficiency and energy loss coefficient of SC at node i when the initial water-temperature $T_{\mathrm{SC},i}^{\mathrm{init}}$ is equal to the daily mean ambient-temperature $\overline{T_{a}}$. $\sum_{t=1}^{N_{\Delta t}}I_{i}^{t}$ is the total solar irradiation throughout the day.

(2) Heat-electric coupling equipment

Two common heat-electric coupling equipment, the gas turbine CHP and EB, are considered in this study. The models are as follows:

$$H_{\mathrm{CHP},i}^{t}=\alpha_{\mathrm{CHP},i}P_{\mathrm{CHP},i}^{t} \tag{37}$$

$$0\leq P_{\mathrm{CHP},i}^{t}\leq P_{\mathrm{CHP},i}^{\max} \tag{38}$$

$$H_{\mathrm{EB},i}^{t}=\eta_{\mathrm{EB},i}P_{\mathrm{EB},i}^{t} \tag{39}$$

$$0\leq H_{\mathrm{EB},i}^{t}\leq H_{\mathrm{EB},i}^{\max} \tag{40}$$

(3) Energy storage equipment

Two forms of energy storage equipment, EES and TES, are taken into account. The general EES model is as follows [40]:

$$S_{\mathrm{EES},i}^{\min}Cap_{\mathrm{EES},i}\leq W_{\mathrm{EES},i}^{t}\leq S_{\mathrm{EES},i}^{\max}Cap_{\mathrm{EES},i} \tag{41}$$

$$0\leq P_{\mathrm{EES,C},i}^{t}\leq \gamma_{\mathrm{EES,C},i}(1-e_{\mathrm{EES},i}^{t})Cap_{\mathrm{EES},i} \tag{42}$$

$$0\leq P_{\mathrm{EES,D},i}^{t}\leq \gamma_{\mathrm{EES,D},i}e_{\mathrm{EES},i}^{t}Cap_{\mathrm{EES},i} \tag{43}$$

$$W_{\mathrm{EES},i}^{t}=W_{\mathrm{EES},i}^{t-\Delta t}(1-\sigma_{\mathrm{EES},i})+(P_{\mathrm{EES,C},i}^{t}\eta_{\mathrm{EES,C},i}-P_{\mathrm{EES,D},i}^{t}/\eta_{\mathrm{EES,D},i})\Delta t \tag{44}$$

$$W_{\mathrm{EES},i}^{t_{\mathrm{end}}}=W_{\mathrm{EES},i}^{0} \tag{45}$$

The general TES model is as follows [41,42]:

$$S_{\mathrm{TES},i}^{\min}Cap_{\mathrm{TES},i}\leq W_{\mathrm{TES},i}^{t}\leq S_{\mathrm{TES},i}^{\max}Cap_{\mathrm{TES},i} \tag{46}$$

$$0\leq H_{\mathrm{TES,C},i}^{t}\Delta t\leq \gamma_{\mathrm{TES,C},i}(1-e_{\mathrm{TES},i}^{t})Cap_{\mathrm{TES},i} \tag{47}$$

$$0\leq H_{\mathrm{TES,D},i}^{t}\Delta t\leq \gamma_{\mathrm{TES,D},i}e_{\mathrm{TES},i}^{t}Cap_{\mathrm{TES},i} \tag{48}$$

$$W_{\mathrm{TES},i}^{t}=W_{\mathrm{TES},i}^{t-1}(1-\sigma_{\mathrm{TES},i})+(H_{\mathrm{TES,C},i}^{t}\eta_{\mathrm{TES,C},i}-H_{\mathrm{TES,D},i}^{t}/\eta_{\mathrm{TES,D},i})\Delta t \tag{49}$$

$$W_{\mathrm{TES},i}^{t_{\mathrm{end}}}=W_{\mathrm{TES},i}^{0} \tag{50}$$

3. Indicators and assessment model of solar energy accommodation capacity in DEHIES

3.1. Indicators

The specific indicators of solar energy accommodation capacity are established from the perspective of the supply side of energy generation in the system on an annual basis considering the variation of solar irradiation and ambient temperature. In order to take into account the energy grade difference of electricity and heat, the energy quality coefficient (EQC) proposed in the Ref. [27] is introduced. The following indicator of annual solar energy accommodation capacity (ASEAC) is established from the perspective of energy supply:

$$\text{ASEAC}=\sum_{d=1}^{N_{\text{day}}}\sum_{t=1}^{N_{\Delta t}}[\sum_{i=1}^{N_{\text{bus}}}P_{\text{PV},i}^{t,d}+\sum_{i=1}^{N_{\text{node}}}\kappa_i^{t,d}H_{\text{SC},i}^{t,d}]\Delta t \tag{51}$$

where $\kappa_i^{t,d}$ is the EQC of hot water heated by the SC at node i and time t on day d, which can be calculated as follows:

$$\kappa_i^{t,d}=1-\frac{T_{\text{a}}^{t,d}}{T_i^{\text{s},t,d}-T_i^{\text{r},t,d}}\ln(\frac{T_i^{\text{s},t,d}}{T_i^{\text{r},t,d}}) \tag{52}$$

Maintaining a reasonable solar curtailment rate can help improve the ASEAC of the DIEHS. A low solar curtailment rate may result in the insufficient installation of solar energy equipment and a waste of solar energy resources. While a high solar curtailment rate may weaken the utilization rate of solar energy equipment. To further study the impact of the solar curtailment rate on the ASEAC, an indicator of the annual solar curtailment rate based on the integrated solar energy accommodation in form of electricity and heat is developed, namely the proportion of annual curtailed electricity and heat in the annual maximum energy supplied by the solar energy equipment of the system considering the energy quality:

$$R_{\text{cur}}^{\text{ann}}=\frac{\text{ASEC}}{\text{ASEAC+ASEC}}\times 100\% \tag{53}$$

where ASEC is the annual solar energy curtailment of the system:

$$\text{ASEC}=\sum_{d=1}^{N_{\text{day}}}\sum_{t=1}^{N_{\Delta t}}[\sum_{i=1}^{N_{\text{bus}}}P_{\text{cur},i}^{t,d}+\sum_{i=1}^{N_{\text{node}}}\kappa_i^{t,d}H_{\text{cur},i}^{t,d}]\Delta t \tag{54}$$

3.2. Assessment model of solar energy accommodation capacity of DIEHS

According to the indicators proposed in 3.1, the assessment of solar energy accommodation capability is aimed at investigating the optimal configuration and operation scheme of solar energy equipment with comprehensive consideration of characteristics of energy networks and various means of improving the ASEAC by maximizing the ASEAC of the DIEHS, and providing the model to evaluate the effect of the typical means like energy storage equipment on the ASEAC improvement. However, a simplistic pursuit of the ASEAC may lead to high power loss, high heat loss, and high solar curtailment rate. To take the green energy-saving principle into account and enhance energy utilization efficiency, it is necessary to consider the suppression of power loss, heat loss, and solar curtailment in the assessment model. As the assessment of solar energy accommodation does not involve the economic factors in this study, the impact of costs on the system is not investigated.

Considering the discussion above, the solar energy accommodation capability of a DIEHS is assessed on an annual basis. The objective function is as follows:

$$\max_{x}\ \text{ASEAC}-\mu_{\text{solar}}\text{ASEC}-\sum_{d=1}^{N_{\text{day}}}\sum_{t=1}^{N_{\Delta t}}[\mu_{\text{loss}}^{\text{e}}\sum_{b=1}^{N_{\text{branch}}}P_{\text{loss},b}^{t,d}+\mu_{\text{loss}}^{\text{h}}\sum_{p=1}^{N_{\text{pipe}}}\kappa_p^{t,d}H_{\text{loss},p}^{t,d}]\Delta t \tag{55}$$

Optimization variable x contains allocation variables and operation variables. Allocation variables consist of the installation area of PV and SC, namely A_{PV} and A_{SC}. Operation variables contain the output and the operation state of the equipment and the grid, and the voltage, current, active and reactive

power, temperature, contains P^t_{grid}, P^t_{PV}, P^t_{cur}, P^t_{CHP}, $P^t_{\text{EES,C}}$, $P^t_{\text{EES,D}}$, e^t_{EES}, W^t_{EES}, H^t_{SC}, H^t_{cur}, H^t_{GB}, H^t_{EB}, $H^t_{\text{TES,C}}$, $H^t_{\text{TES,D}}$, e^t_{TES}, W^t_{TES}, u^t, i^t, P^t, Q^t, P^t_i, Q^t_i, $T^{\text{s},t}$, $T^{\text{r},t}$, H^t_{source}. Except for the charge and discharge state of the energy storage equipment, e^t_{EES} and e^t_{TES}, which are 0-1 integer variables, the other optimization variables are all of double. The control variables include $P^t_{\text{loss},ij}$, $H^t_{\text{loss},ij}$, ASEAC and ASEC, which are both of double.

The constraints of the assessment model contain the operation of the DHN and PDN, solar energy equipment, heat-electric coupling equipment, and energy storage equipment, namely Eqs. (11)–(12), Eqs. (14)–(26) , Eqs. (28)–(35), Eqs. (37)–(50)).

To simplify the calculation, $T^{\text{s},t}_i$ and $T^{\text{r},t}$ in the calculation formula of EQC, Eq. (52), are replaced with the average temperature of the operating temperature range of supply and return pipelines. The entire model for the assessment of the solar energy accommodation capability of the DIEHS is then a 0-1 mixed-integer linear program, which can be solved by existing optimization solvers, such as YALMIP and CPLEX.

4. Case Study

The assessment model of solar energy accommodation is validated through a case study conducted on the DIEHS consisting of the IEEE 33-bus system and a DHN of Jilin Province in China [30]. The assessment is based on three kinds of typical days in winter, the transition season, and summer, and the numbers of three seasons are assumed to be 120, 153, and 92, respectively. The operation interval is 15 min.

The layout of the DIEHS in the case study is shown in Appendix (Fig. A1). The system contains two energy stations and both include PVs, SCs, CHP units, and EBs. The parameters of the energy stations, the main grid, and the penalty coefficients are shown in Appendix (Table A1) [43]. The parameters of the DHN can be found in [30]. The electrical and heat load are selected for a typical industrial area (Fig. A2). The typical solar irradiance intensity and ambience temperature curves are given in in Appendix (Fig. A3). The operating ranges of the supply and return temperatures in the entire DHN are 90–110 °C and 70–90 °C, respectively. The initial temperature of the tank of SCs on three typical days are set to 100 °C. As the distributed energy supply equipment affects the system operation and analysis by changing the local energy demand, the case study focuses on the centralized energy supply of the energy station rather than its distributed energy supply.

4.1. Case 1: Impact of the transmission delay of the DHN

To explore the influence of a transmission delay of the DHN on solar energy accommodation, the model proposed above is used to assess the solar energy accommodation capability of a DIEHS in cases where the transmission delay of the DHN is ignored and considered. To stress the influence of the transmission delay of the DHN, solar curtailment is not allowed to occur and the capacities of storage equipment are set to 0. The optimal results of the two cases are shown in Table 1.

Table 1 Optimal result when ignoring/considering the transmission delay

Case	Case 1.1: Ignoring transmission delay	Case 1.2: Considering transmission delay
Area of PV (m^2)	16731.11	14943.47
Area of SC (m^2)	3268.89	5056.53
ASEAC (kWh)	12614745.42	14053500.35
Power loss (kWh)	7912.61	8309.05
Heat loss (kWh)	11202.56	11243.03

A comparison of the optimal result when considering the transmission delay of the DHN to the result when the transmission delay is ignored revealed that the installation area of SC increased by 54.7% and

the area of the PV reduced by 10.7%. The ASEAC increased by 11.4%. The change mentioned above occurs because the efficiency of the SC is larger than that of PV, and the ASEAC of the system is greater by installing SCs in the same area. This result reveals that the solar energy accommodation capability can be improved without sacrificing operation safety by increasing the installation area of the SC. Fig. 4 shows the thermal scheduling strategy of energy stations on three typical days when ignoring (a) and considering (b) the transmission delay. When the transmission delay is not considered (a), the balance of heat load, heat loss, and heat supply is maintained at all times. At this point, the key restriction of more SC installations is the heat load at noon. When considering the transmission delay of the DHN, the output of the heat sources can exceed the heat load restriction and ensures operation safety at the same time, which results in an increase in SC installations. And the thermal output of the ESs increases during the noon period when the solar irradiation is strongest but not the time before peak demand to accommodate more solar energy. The exceeded amount of thermal output just causes a little increase of 40.47 kWh in the annual heat loss thanks to the heat loss penalty term, and the increased ASEAC of 1438754.93 kWh is much more.

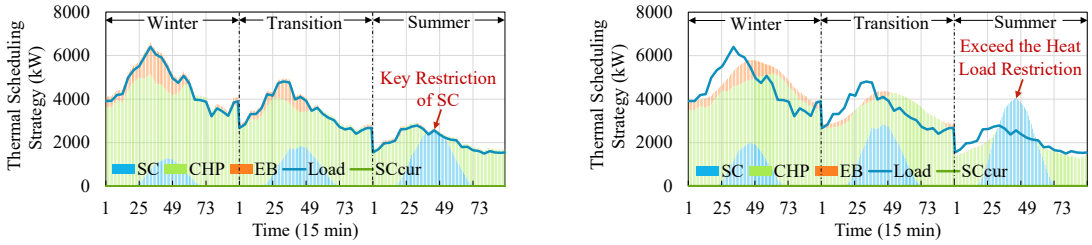

(a) Ignoring transmission delay (b) Considering transmission delay

Fig. 4. Thermal scheduling strategy of energy stations when ignoring/considering transmission delay

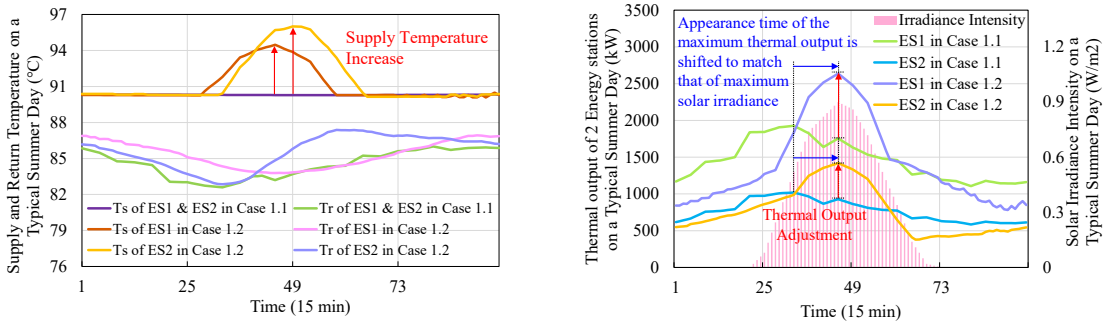

(a) (b)

Fig. 5. Supply/return temperature (a) and thermal output (b) of two ESs on a typical summer day when ignoring/considering transmission delay

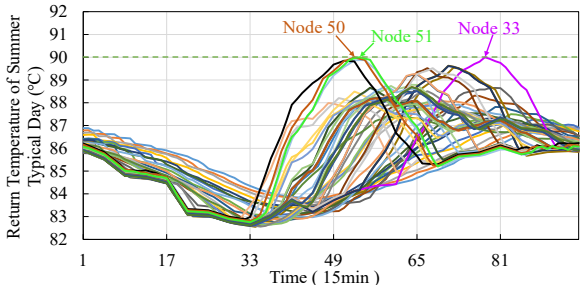

Fig. 6. Return temperature on a typical summer when considering transmission delay

The reason for the output of heat source exceeding the heat load restriction when considering transmission delay of the DHN can be summarized as two:

(1) The appearance time of the peak thermal output can be controlled to match the peak time of the solar irradiance intensity is highest (shown as the blue arrows in Fig. 5 (b)) by adjusting the supply

temperatures of the energy stations, owing to a certain time delay for return temperatures compared to the supply temperatures, which leaves more room for the energy supply of the SCs.

(2) The peak value of the thermal outputs can be further increased (shown as "Thermal Output Adjustment" in Fig. 5 (b)) by raising the supply temperature within a reasonable range (shown as "Supply Temperature Raise" in Fig. 5 (a)), which can help to accommodate more SC heating.

However, the increase in the thermal outputs of the energy stations is limited by the operating range of the return temperatures in the DHN. Fig. 6 shows the return temperatures of all nodes on a typical summer day when considering the transmission delay. Owing to the low heat load and the small temperature difference between supply and return pipelines in the summer period, the increase in the supply temperatures of the energy stations results in the return temperatures of nodes 33, 50, and 51 reaching the upper limit of 90 °C sometimes, and the peak thermal outputs of the energy stations reach their limits.

4.2. Case 2: Impact of the operating temperature range on solar energy accommodation

It can be known from Case 1 that the solar energy accommodation capability is limited by the operating temperature range of return pipelines, especially the upper limit of the return temperature, T_r^{max}. In Case 2, the upper limit of the return temperature is adjusted to within 85–100 °C to study the influence of the operating temperature range on the ASEAC of the system. To stress the influence of the operating temperature range, solar curtailment is not allowed to occur and the capacities of storage equipment are set to 0.

The optimal results with different T_r^{max} are shown as Fig. 7. With an increase in T_r^{max}, the installed area of SC and ASEAC increase gradually, and the growth slows down gradually when T_r^{max} exceeds 94 °C. While the installation of PV changes with an opposite tendency. Besides, the system cannot operate normally when T_r^{max} is lower than 87 °C.

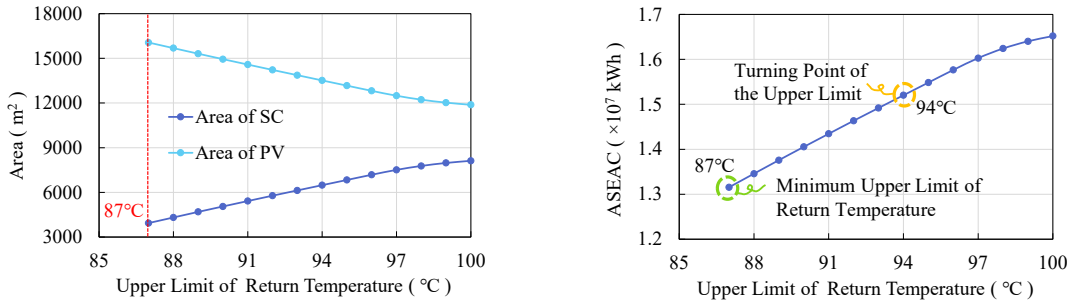

(a) (b)

Fig. 7. Optimal results of the total capacity of SC/PV (a) and annual accommodated solar energy (b) with variation in the upper limit of the return temperature

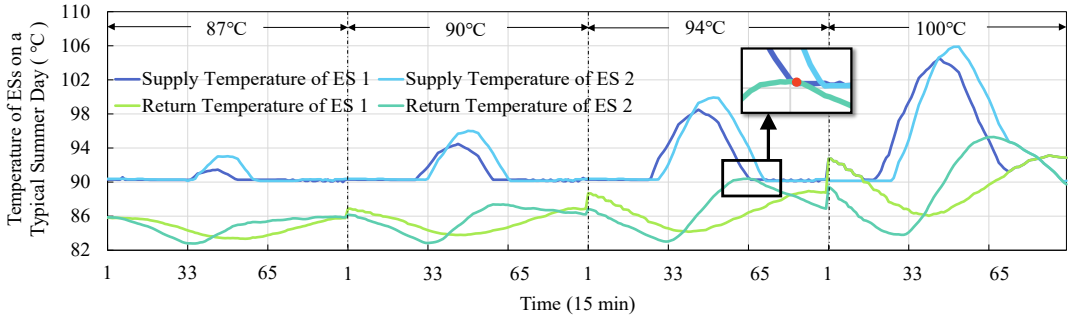

Fig. 8. Supply and return temperatures of energy stations on a typical summer day when the upper limit of the return temperature controlled at 87 °C, 90 °C, 94 °C, 100 °C

The reasons for the results above are further analyzed through Fig. 8, the supply and return temperature curves of energy stations on a typical summer day with T_r^{max} controlled at 87 °C, 90 °C, 94 °C, 100 °C, respectively. With an increase in T_r^{max}, the supply and return temperatures of the energy stations increase in the daytime. From 94 °C, the temperature difference between the supply and return pipelines decreases such that the two temperature curves overlap (shown as the red points in Fig. 8), which causes a slow growth of the SC installation. With a further increase in T_r^{max}, the time period during which the supply and return temperature curves of the energy stations coincide continuously increases (shown as the temperature curve with T_r^{max} of 100 °C in Fig. 8), which leads to a more obvious slowing growth of the SC installation and ASEAC.

Due to the heat load and the lower limit of the supply temperature, T_r^{max} has a minimum value, which is 87 °C in this case. Fig. 9 shows the temperature curves with T_r^{max} of 87 °C. It can be seen that there are always some nodes whose supply temperatures reach the lower limit of 90 °C at every time point. If T_r^{max} further decreases, the supply temperature of some nodes will be lower than the allowable lower limit of 90 °C, which indicates that the operating temperature constraints of the system are exceeded.

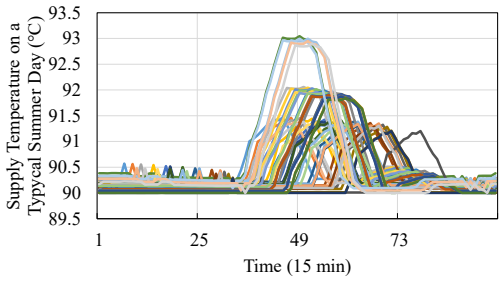

Fig. 9. Supply temperature on a typical summer day

4.3. Case 3: Impact of solar curtailment on solar energy accommodation

In both academia and industry, there has been a lack of consensus on suitable approaches for maintaining a reasonable solar curtailment rate in solar energy accommodation. In Case 3, the solar curtailment penalty coefficient is adjusted within 0.0001–1000 to study the variation in the installation of solar energy equipment and ASEAC under different solar curtailment rates, R_{cur}^{ann}. To put aside the influence of energy storage equipment, the capacities of storage equipment are set to 0 in Case 3.

Fig. 10 shows the optimal results under different R_{cur}^{ann}. With an increase in R_{cur}^{ann}, the installation area of SC and ASEAC increase gradually and approach a saturated value (shown as the yellow dotted line in Fig. 10 (b)). The results reveal that an appropriate increase in SC installation will cause the phenomenon of solar curtailment, but it will also help to increase the ASEAC of the system. However, the excessive installation area of SC may lead to excessive curtailment of solar energy, resulting in an unnecessary waste of resources. In this case, the improvement of ASEAC begins to slow down significantly when R_{cur}^{ann} exceeds 11.03%. Therefore, it is more reasonable to control R_{cur}^{ann} below 11.03%.

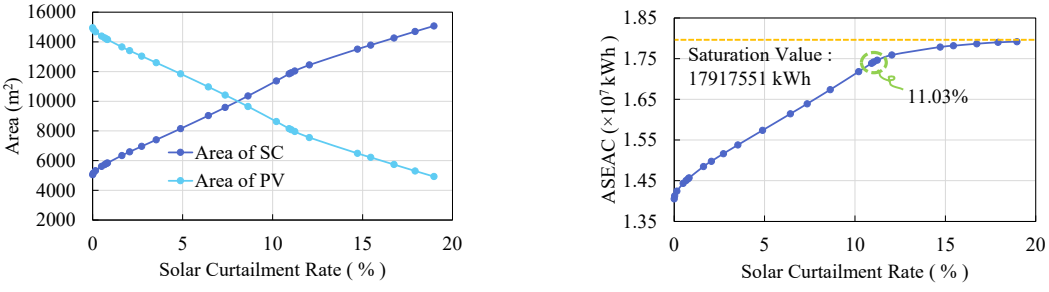

Fig. 10. Optimal results of SC/PV installation (a) and annual accommodated solar energy (b)

The saturated value of ASEAC is mainly affected by the return temperature. Fig. 11 shows the supply temperature curves of the two energy stations under different R_{cur}^{ann}. Fig. 12 shows the return temperature curves of all nodes with R_{cur}^{ann} of 0, 4.89%, 11.03%, 18.96%, respectively. To further improve the solar energy accommodation capability of the system, the supply temperature of the energy stations will be raised continuously to provide more accommodation space for the SC (Fig. 11). However, restricted by the upper limit of the return temperatures, the supply temperatures of the energy stations cannot be raised infinitely, which further limits the thermal output of the SC. Therefore, the improvement in ASEAC needs to be realized by an appropriate amount of solar energy curtailment of the SC to meet the operating temperature constraints. The larger the area of installed SCs, the greater the nodes whose return temperatures reach the upper limit, and the longer the temperatures are maintained at the return temperature upper limit (Fig. 12). At the same time, the time for the supply temperatures of the energy stations reaching "the ceiling" (Fig. 11) is longer, and R_{cur}^{ann} increases, resulting in ASEAC approaching the saturated value.

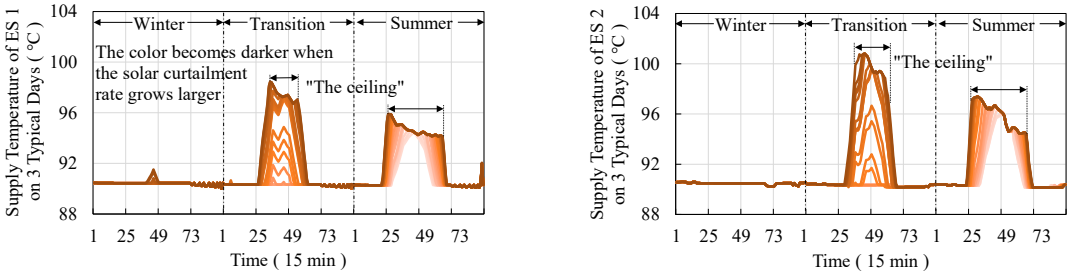

(a) Energy station 1 (b) Energy station 2

Fig. 11. Supply temperatures of the energy stations on three typical days (The color becomes darker when the solar curtailment penalty coefficient increases)

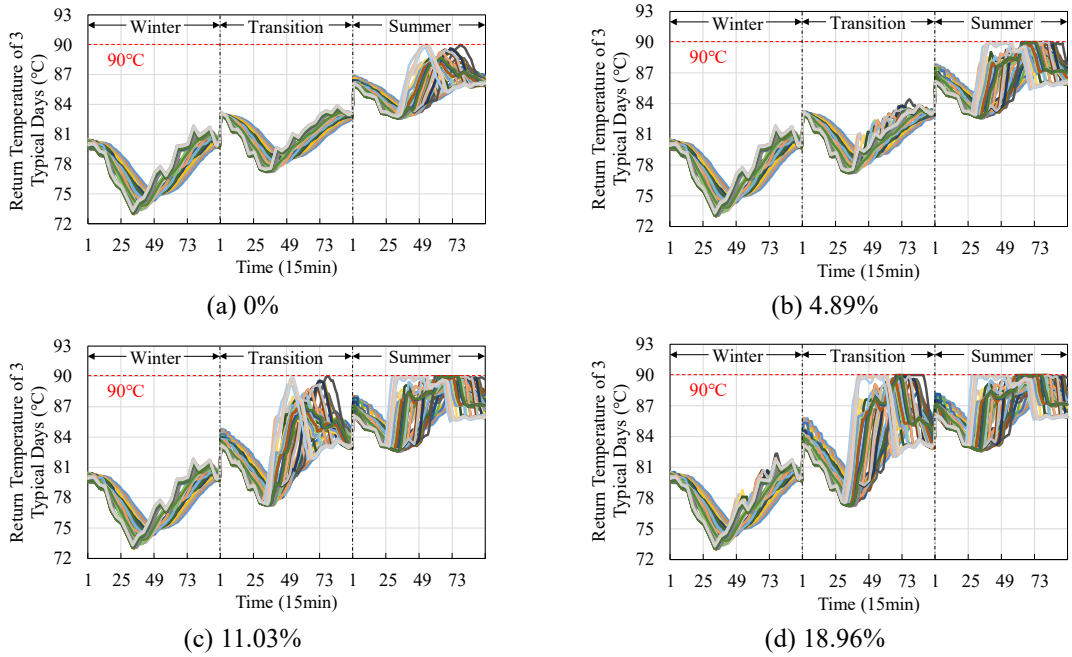

(a) 0% (b) 4.89%

(c) 11.03% (d) 18.96%

Fig. 12. Return temperatures of all nodes when the curtailment rate is 0 (a), 4.89% (b), 11.03% (c), and 18.96% (d)

To use solar energy more reasonably, the economic factor of solar energy accommodation needs to be considered. Therefore, the variation in the annual net revenue under different R_{cur}^{ann} is analyzed next. The annual net revenue refers to the difference between the income from the sale of energy to users and

the sum of the energy purchase cost and the annual investment costs of the PV and SC. Let us assume that the investment costs of the PV and SC are 2609 RMB/m^2、1400 RMB/m^2, respectively, and the purchase price of gas is 2.66 RMB/m^3 and the purchase price of electricity from the grid is 0.5 RMB/kWh. Furthermore, the discount rate is 0.06, and the service lives of the PV and SC are both 10 years.

Fig. 13 shows increases in annual net revenue under different R_{cur}^{ann} from the baseline situation with no solar curtailment. The increase in annual net revenue is largest when R_{cur}^{ann} is 2.72% (shown as the red point marked in Fig. 13). The annual net revenue of the situation with R_{cur}^{ann} of 8.04% is equal to the situation with no solar curtailment (shown as the yellow point in Fig. 13), but ASEAC increased by 17.87%, which can be calculated from Fig. 10 (b). A further increase in R_{cur}^{ann} will decrease the annual net revenue compared to the situation of no solar curtailment. Therefore, considering the economy and solar energy accommodation capability of the system comprehensively, R_{cur}^{ann} should be controlled between 2.72%~8.04% in this case.

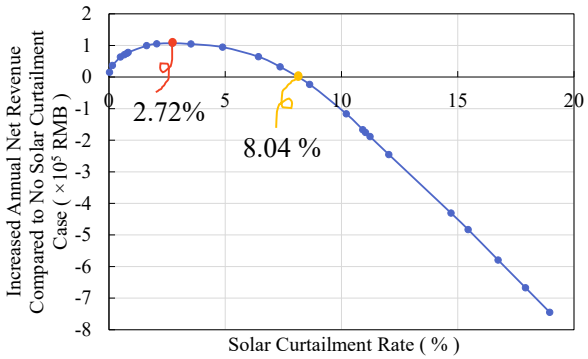

Fig. 13. Increases in annual net revenue compared to the no solar curtailment case

4.4. Case 4: Impact of the energy storage on solar energy accommodation

To study the impact of the EES and TES on the solar energy accommodation capability of the system, four subcases are set up and the setting of each can be found in Table 2. The parameters of the energy storage equipment are shown in Appendix (Table A2). Solar curtailment is not allowed to occur in Subcases as it would have impacted the analysis.

The optimal results of the four subcases are shown in Table 3. Comparing the optimal result of Case 4.1 with that of Case 4.2 and the optimal result of Case 4.3 with that of Case 4.4, it can be found that the EES has almost no effect on the solar energy accommodation capability of the system because the SC plays a dominant role in solar energy accommodation and the EES does not interfere with the operation of DHN directly. Furthermore, comparisons of the optimal results of Case 4.1 with that of Case 4.3 and the optimal result of Case 4.2 with that of Case 4.4 reveal that installing the TES of 4000 kW can increase the annual solar energy accommodated by 3.69%.

Table 2 Subcase setting of Case 4

Case	Case 4.1	Case 4.2	Case 4.3	Case 4.4
Capacity of EES (kW)	0	10000	0	10000
Capacity of TES (kW)	0	0	4000	4000

Table 3 Optimal results of Case 4.1–Case 4.4

	Case 4.1	Case 4.2	Case 4.3	Case 4.4
Area of PV (m^2)	14943.47	14943.47	14298.77	14298.73
Area of SC (m^2)	5056.53	5056.53	5701.23	5701.26
ASEAC (kWh)	14053500.35	14053500.28	14572676.02	14572649.83

To further analyze the effect of TES on the solar energy accommodation capability of the system, the optimal results of different TES capacities without considering the solar energy curtailment and EES are obtained (Fig. 14). With an increase in TES capacity, the installation of SC and ASEAC increase gradually. Fig. 15 shows the thermal scheduling strategy of energy stations with TES capacities of 0, 4000 kW, 10000 kW, and 20000 kW on a typical summer day. With an increase in TES capacity, the heat charged by the TES increases during the noon period to improve the thermal output of the SC and thereby the solar energy accommodation capability.

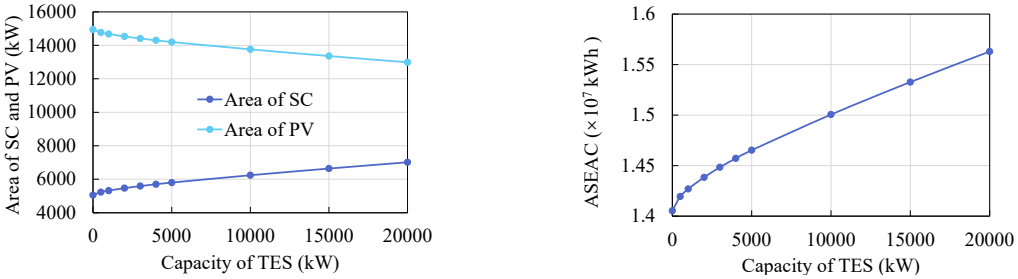

Fig. 14. Optimal result of the total capacity of SC/PV (a) and annual accommodated solar energy of (b) with an increase in TES capacity with no solar energy curtailment

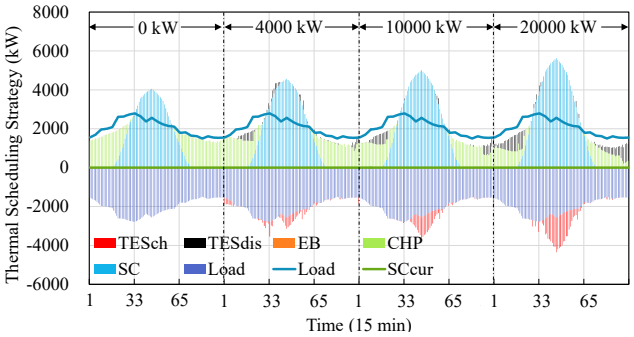

Fig. 15. Thermal scheduling strategy of energy stations on a summer typical day with the TES capacity of 0, 4000 kW, 10000 kW, and 20000 kW with no solar energy curtailment

Fig. 16 shows the supply temperature curves of energy stations on a typical summer day with TES capacity of 0, 4000 kW, 10000 kW, and 20000 kW, respectively, which reveals the relationship between the effect of the TES and solar energy curtailment on the solar energy accommodation capability. With an increase in TES capacity, the supply temperature curves of the energy stations are more similar to those of Case 3. Furthermore, "the temperature ceiling" appears in both Fig. 11 and Fig. 16. This is because the TES can store the solar energy that needs to be curtailed to improve the solar energy accommodation capability. Therefore, the TES is generally regarded as an important means for improving the solar energy accommodation capability and solving the problem of solar curtailment.

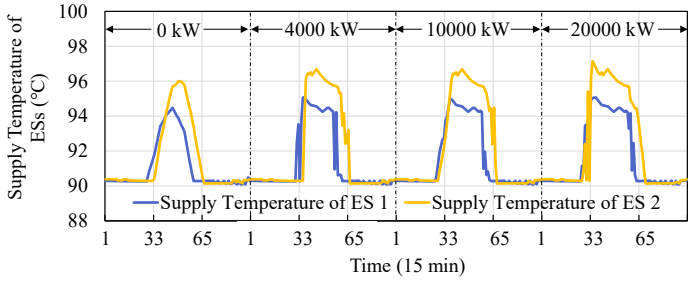

Fig. 16. Supply temperatures of the energy stations on a typical summer day with TES capacity of 0, 4000 kW, 10000 kW, and 20000 kW when considering the solar energy curtailment

5. Conclusions

Considering the solar accommodation forms of electric and thermal energy, indicators and an assessment model for the solar energy accommodation capability in a DIEHS is developed based on the energy grades of electricity and heat, and the transmission delay of the DHN and operation security are taken into account. The model can help to determine the maximum solar energy accommodation potential of the target system and provide a corresponding optimal solar energy accommodation scheme. Effective approaches to improving the solar energy accommodation capacity are investigated through a case of a DIEHS consisting of an IEEE 33-bus system and a DHN of China, which can provide reference for further improvement of solar energy accommodation. The conclusions are as follows:

(1) SCs plays a crucial role in enhancing the solar energy accommodation capability. The transmission delay characteristics of the DHN can be fully utilized by adjusting the supply temperature of energy stations in a reasonable range to exceed the restriction of the heat load on a typical summer day. The peak thermal output of the energy stations can be further increased owing to the match of the appearance time of the peak thermal output with the time when the solar irradiance intensity is highest, which leads to further improvement of the ASEAC.

(2) An increase in the upper limit of return temperature within a reasonable range can promote the ASEAC of the DIEHS. Meanwhile, the minimum upper limit of the return temperature can be limited by the heat load and the lower limit of supply temperature.

(3) An appropriate increase in SC capacity will cause the phenomenon of solar curtailment, but it will also help to promote solar energy accommodation. Maintaining a reasonable solar curtailment rate contributes to a larger annual net revenue while the ASEAC is improved.

(4) For the system in which the SC plays a dominant role in solar energy accommodation, the influence of the TES on the ASEAC is more significant than that of the EES. Besides, the TES is regarded as an important method for improving solar energy accommodation capability and dealing with solar energy curtailment.

Our future research will explore the influence of integrated demand response and the interaction between sources and users on solar energy accommodation capability. In addition, the uncertainty of solar energy will be considered in the assessment of solar energy accommodation

Acknowledgements

This work was financially supported by the Joint Fund Project of National Natural Science Foundation- State Grid Corporation (Grant no. U1766210).

Appendix

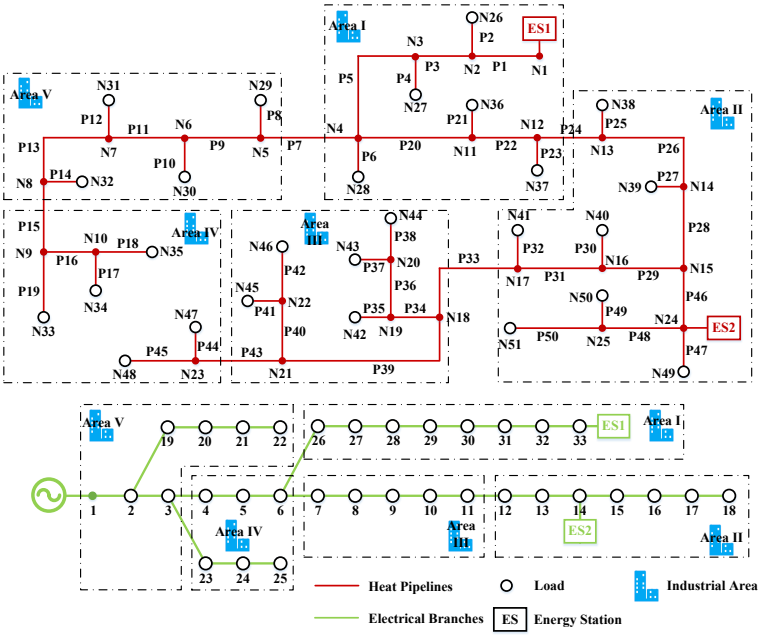

Fig. A1. Case layout of the district heat-electric coupling integrated energy system

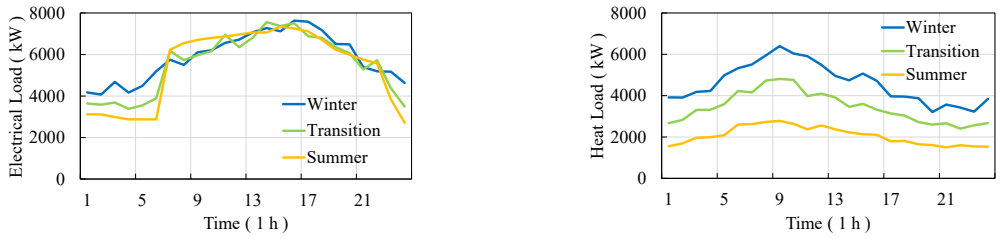

(a) (b)

Fig. A2. Electrical load (a) and heat load (b) of three typical days for a typical industrial area

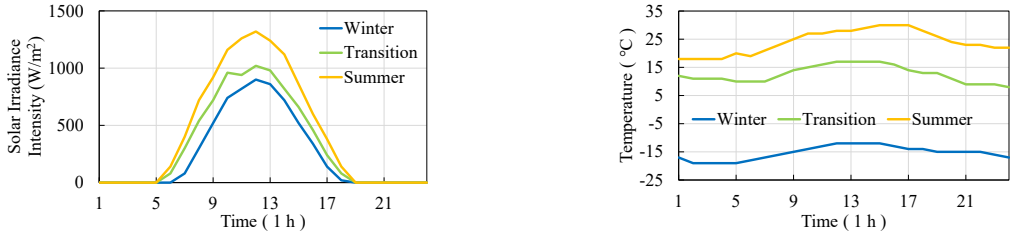

(a) (b)

Fig. A3. Solar irradiance intensity (a) and ambience temperature (b) on three typical days

Table A1 Parameters of the energy stations, the main grid, and the penalty coefficients [43]

Parameters	Value	Parameters	Value	Parameters	Value	Parameters	Value
$A^{\max}$ (m^2)	10000	η_{PV}	0.175	η^{*}_{SC}	0.726	U_{loss} (℃·m^2/W)	4.86
η_{CHP}	0.35	α_{CHP}	1.43	η_{EB}	0.9	$P^{\max}_{gird}$ (kW)	8000
$P^{\max}_{CHP}$ (kW)	5000	$H^{\max}_{EB}$ (kW)	5000	μ_{solar}	100	μ^{e}_{loss} 、 μ^{h}_{loss}	1

Table A2 Parameters of the energy storage equipment in Case 4

Parameters	Value	Parameters	Value	Parameters	Value	Parameters	Value
$\eta_{EES,C}$ / $\eta_{EES,D}$	0.95	$S^{0}_{EES,C}$	0.5	$\eta_{TES,C}$ / $\eta_{TES,D}$	0.99	$S^{0}_{TES,C}$	0.5
$\gamma_{EES,C}$ / $\gamma_{EES,D}$	0.2	$S^{\max}_{EES,C}$	0.9	$\gamma_{TES,C}$ / $\gamma_{TES,D}$	0.5	$S^{\max}_{TES,C}$	0.9
σ_{EES}	0.04	$S^{\min}_{EES,C}$	0.2	σ_{TES}	0.0001	$S^{\min}_{TES,C}$	0.2

Nomenclature

Nomenclature		κ	EQC (-)
Symbols and Sets		S	Storage rate of EES or TES (-)
P / Q	Active power (kW) / reactive power (kVar)	γ	Charging or discharging rate of EES or TES (-)
i / u	Square of current (A^2) / voltage (V^2)	μ	Penalty coefficient (-)
T	Temperature (°C)	$\boldsymbol{N}$	Numbers of branches / pipes / days
H	Heat power (kW)	*Superscript*	
W	Stored energy of EES or TES (kWh)	t	Time
e	Storage state of EES or TES (0/1)	init / end	Initial / last dispatch time of a day
A	Installation area (m^2)	ann	Annual
E	Energy (kWh)	s / r	Supply / return pipelines
R	Solar energy curtailment rate (-)	e / h	Electrical / heat
δ	Set of upstream pipes or branches	max / min	maximum / minimum
ζ	Set of downstream pipes or branches	*Subscript*	
Parameters		grid	The grid
m	Mass flow (kg/s)	PV	Photovoltaic
β	Mass flow distribution coefficient (-)	SC	Solar collector
τ	The number of time interval (-)	CHP	Combined power and heat
Δt	Time interval (15 min)	EB	Electric boiler
l	Pipe length (m)	TES / EES	Thermal / electric energy storage
Δl	Length interval (-)	D / C	Discharge / charge
D	Diameter (m)	cur	Curtailment
ρ	Density of hot water	source	Heat source
λ	Heat transfer coefficient (W/(m·K))	load	Electrical or heat load
r / x	Impedance (Ω)	out	Outlet of pipes
I	Solar irradiance intensity (kW/m^2)	loss	Electrical or heat loss
Cap	Capacity of equipment (kW)	a	Ambiance
η	Efficiency of equipment (-)	solar	Solar energy
U	Energy loss coefficient of the SC (-)	i / j / k	Node or bus i / j / k
α	Heat-to-power ratio (-)	ij / jk	Pipe ij or branch ij / jk
σ	Loss rate of EES / TES (-)	d	Typical day d

References

[1] Brunet C, Savadogo O, Baptiste P, Bouchard MA. Shedding some light on photovoltaic solar energy in Africa – A literature review. Renew Sustain Energ Rev 2018; 96:325-42.

[2] Hosseini SE, Wahid MA. Hydrogen from solar energy; a clean energy carrier from a sustainable source of energy. Int J of Energ Res 2019; 44(6):4110-4131.

[3] British Petroleum (BP). Statistical review of world energy 2020, https://www.bp.com/statisticalreview; 2020 [accessed 24 Jul 2020].

[4] Liu P, Chu P. Wind power and photovoltaic power: How to improve the accommodation capability of renewable electricity generation in China?. Int J Energ Res 2018; 42:2320-2343.

[5] Raimon OB, Numan SC. Comprehensive overview of optimizing PV-DG allocation in power system and solar energy resource potential assessments. Energ Rep 2020; 6:173-208.

[6] Zhang Y, Ren J, Pu Y, Wang P. Solar energy potential assessment: A framework to integrate

geographic, technological, and economic indices for a potential analysis. Renew Energ 2020; 149:577-586.

[7] Mahtta R, Joshi PK, Jindal AK. Solar power potential mapping in India using remote sensing inputs and environmental parameters. Renew Energ 2014; 71:255-262.

[8] You W, Geng Y, Dong H, Wilson J, Pan H, Wu R, Sun L, Zhang X, Liu Z. Technical and economic assessment of RES penetration by modelling China's existing energy system. Energy 2018; 165:900-910.

[9] Wang L, Li X. Study on the accommodating capability of large-capacity grid-connected photovoltaic generation system. IEEE Advanced Information Management, Communicates, Electronic and Automation Control Conference (IMCEC); 2016. p. 1261-1265.

[10] International Renewable Energy Agency (IRENA). Global renewables outlook: energy transformation 2050, https://www.irena.org/publications/2020/Apr/Global-Renewables-Outlook-2020; 2020 [accessed 24 Jul 2020].

[11] Carpaneto E, Lazzeroni P, Repetto M. Optimal integration of solar energy in a district heating network. Renew Energ 2015; 75:714-721.

[12] Popovski E, Aydemir A, Fleiter T, Bellstädt D, Büchele R, Steinbach J. The role and costs of large-scale heat pumps in decarbonising existing district heating networks – A case study for the city of Herten in Germany. Energy 2019; 180:918-933.

[13] Fu H, Zhao X, Ma L, Zhang T, Wu Q, Sun H. A comparative study on three types of solar utilization technologies for buildings: Photovoltaic, solar thermal and hybrid photovoltaic/thermal systems. Energ Convers Manag 2017; 140:1-13.

[14] Li D, Chong B, Chan W, Lam J. An analysis of potential applications of wide-scale solar energy in Hong Kong. Build Serv Eng Res T 2014; 35(5): 516-528

[15] Groppi D, de Santoli L, Cumo F, Garcia DA. A GIS-based model to assess buildings energy consumption and usable solar energy potential in urban areas. Sustain Cities Soc 2018:40: 546-558.

[16] J Wu, J Yan, Jia H, Hatziargyriou N, Djilali N, Sun H. Integrated Energy Systems. Appl Energ 2016; 167:155-157.

[17] Masood P, Henrik WB, Meysam Q. Guest editorial: maximising flexibility through energy systems integration. IET Energ Syst Integr 2020; 2(2): 67-68.

[18] Li Y, Wang C, Li G, Wang J, Zhao D, Chen C. Improving operational flexibility of integrated energy system with uncertain renewable generations considering thermal inertia of buildings. Energ Convers Manag 2020; 207:112526.

[19] Li J, Fang J, Zeng Q, Chen Z. Optimal operation of the integrated electrical and heating systems to accommodate the intermittent renewable sources. Appl Energ 2015; 167:244-254.

[20] Wei W, Jia H, Mu Y, J Wu, Jia H. A robust assessment model of the solar electrical-thermal energy comprehensive accommodation capability in a district integrated energy system. Energies 2019; 12(7):1363.

[21] Zhang D, Li B, Zhao Q, Li J. Thermal performance and energy characteristic analysis of multiple renewable energy complementary heat pump system. Sol Energ 2020; 196:287-294.

[22] Carpaneto E, Lazzeroni P, Repetto M. Optimal integration of solar energy in a district heating network. Renew Energ 2015; 75:714-721.

[23] Pan Z, Guo Q, Sun H. Interactions of district electricity and heating systems considering time-scale characteristics based on quasi-steady multi-energy flow. Appl Energ 2016; 167:230-243.

[24] Li C, Huang Y, Liu C, Wang Y, Dong C, Liang Z. Research on Evaluation Method of Renewable

Energy Accommodation Capability Based on LSTM. 2018 2nd IEEE Conference on Energy Internet and Energy System Integration (EI2); 2018. p. 1-5.

[25] Li Y, Wei L, Chi Y, Wang Z, Zhang Z. Study on the key factors of regional power grid renewable energy accommodating capability. IEEE PES Asia-Pacific Power and Energy Engineering Conference (APPEEC); 2016. p. 790-794.

[26] Dincer I, Cengel YA. Energy, entropy and exergy concepts and their roles in thermal engineering. Entropy 2001; 3(3):116-149.

[27] Hu X, Zhang H, Chen D, Li Y, Wang L, Zhang F, Cheng H. Multi-objective planning for integrated energy systems considering both exergy efficiency and economy. Energy 2020; 197:e117155.

[28] Wang D, Zhi Y, Jia H, Hou K, Zhang S, Du W, Wang X, Fan M. Optimal scheduling strategy of district integrated heat and power system with wind power and multiple energy stations considering thermal inertia of buildings under different heating regulation modes. Appl Energ 2019; 240: 341-358.

[29] Liu X, Combined analysis of electricity and heat networks. Cardiff: Cardiff University; 2013.

[30] Gu W, Wang J, Lu S, Luo Z, Wu C. Optimal operation for integrated energy system considering thermal inertia of district heating network and buildings. Appl Energ 2017; 199:234-246.

[31] Yu J, Guo L, Ma M, Kamel S, Li W, Song X. Risk assessment of integrated electrical, natural gas and district heating systems considering solar thermal CHP plants and electric boilers. Int J Elec Power 2018; 103:277-287.

[32]. Ministry of Housing and Urban-Rural Development of the People's Republic of China (MOHURD). Design code for city heating network. Beijing: Guangming Daily Press; 2010.

[33] Ru Y, Kleissl J, Martinez S. Storage size determination for grid-connected photovoltaic systems. IEEE Trans Sustain Energ 2013; 4:68-81.

[34] Soteris A. Kalogirou, Solar energy engineering: processes and systems, UK: Academic Press; 2013.

[35] Duffie J, Beckman W, Worek W. Solar engineering of thermal processes. New York: Wiley Interscience Publication; 2006, 116(1):549.

[36] Xu T, Zhang N. Coordinated operation of concentrated solar power and wind resources for the provision of energy and reserve services. IEEE Trans Power Syst 2017; 32(2): 1260-1271.

[37] Huang B, Du S. A performance test method of solar thermosyphon system. ASME J Solar Energy Eng 1991;113:172-9.

[38] Guo C, Ji J, Sun W, Ma J, He W, Wang Y. Numerical simulation and experimental validation of tri-functional photovoltaic/thermal solar collector. Energy 2015; 87:470-480.

[39] Ji J, Lu J, Chow T, He W, Pei G. A sensitivity study of a hybrid photovoltaic/thermal water-heating system with natural circulation. Appl Energ 2007; 84(2):222-237.

[40] Qin M, Chan K, Chung C, Luo X, Wu T. Optimal planning and operation of energy storage systems in radial networks for wind power integration with reserve support. IET Gener Transm Dis 2016; 10(8):2019-2025.

[41] Wang Y, Luo S, Wu Y, Wang S. Flexible operation of retrofitted coal-fired power plants to reduce wind curtailment considering thermal energy storage. IEEE Trans Power Syst 2020; 35(2): 1178-1187.

[42] Liu B, Meng K, Dong Z, Wei, W. Optimal dispatch of coupled electricity and heat system with independent thermal energy storage. IEEE Trans Power Syst 2019; 34(4): 3250-3263.

[43] Hu M, Pei G, Wang Q, Li J, Wang Y, Ji J. Field test and preliminary analysis of a combined diurnal solar heating and nocturnal radiative cooling system. Appl Energ 2016; 179:899-908.

Declaration of interests

☒ **The authors declare that they have no known competing financial interests or personal relationships that could have appeared to influence the work reported in this paper.**

☐The authors declare the following financial interests/personal relationships which may be considered as potential competing interests:

Author Statement

Wei Wei: Conceptualization, Methodology, Validation, Formal analysis, Writing - Original Draft, Writing - Review & Editing

Jingwen Wu: Methodology, Software, Validation, Formal analysis, Writing - Original Draft, Writing - Review & Editing

Yunfei Mu: Writing - Conceptualization, Review & Editing

Jianzhong Wu: Writing - Conceptualization, Review & Editing

Hongjie Jia: Writing - Review & Editing